

Received October 18, 2017, accepted November 21, 2017, date of publication December 8, 2017, date of current version May 2, 2018.

Digital Object Identifier 10.1109/ACCESS.2017.2779453

Degradation Trend Prognostics for Rolling Bearing Using Improved R/S Statistic Model and Fractional Brownian Motion Approach

QING LI¹ , (Graduate Student Member, IEEE), AND STEVEN Y. LIANG^{1,2}

¹College of Mechanical Engineering, Donghua University, Shanghai 201620, China

²George W. Woodruff School of Mechanical Engineering, Georgia Institute of Technology, Atlanta, GA 30332-0405, USA

Corresponding author: Qing Li (suesliqing@163.com)

This work was supported in part by the Fundamental Research Funds for the Central Universities under Grant CUSF-DH-D-2017059 and in part by the Research Funds of Worldtech Transmission Technology under Grant 12966EM.

ABSTRACT Fractional order characteristics (FOCs) have been shown to be useful in the predict degradation trend of rotating machinery. In this paper, a novel prognostics methodology based on improved R/S statistic and fractional Brownian motion (FBM) for rolling bearing degradation process is proposed. Due to the fact that bearing health indicators, such as equivalent vibration intensity (EVI), often exhibit non-stationary and non-Gaussian traits, the FOC methodology normally involves the estimation of a parameter Hurst H; the improved R/S statistic technique with auto-covariance estimator was introduced to address the issue that the calculation of the Hurst exponent by classical R/S methods is sensitive to heteroskedasticity and short-range dependence. Furthermore, a slow degrading process of a rolling bearing can be predicted by a common FOC model, but the actual sharp transition points (STPs) of the degradation are often very difficult to track. The main purpose of a rolling bearing degradation prediction is to prognosticate and track the STP's trend when the failure occurs between the normal phase and the incipient degradation phase. A method that combined FBM and Brownian motion is presented when the forecasted points contaminated with STPs, in which the predicting operator, driven by a new stochastic differential equation and its computationally efficient algorithm, are explored. The experimental results show that the proposed approach can better predict the EVI degradation trend than traditional FOC and other time series models.

INDEX TERMS Fractional Brownian motion (FBM), stochastic differential equation (SDE), Hurst exponent (HE), improved R/S statistic model, degradation trend prognostics.

I. INTRODUCTION

Prognostics and health management (PHM) is of the significance to guarantee safety, reliability and efficiency of mechanical equipment, and has been implemented in various applications such as rolling bearings [1], [2], gear-box [3]–[5], and rotor machinery system [6], [7].

Rolling bearings used in rotating machinery are subjected to harsh working environments, including vibration, corrosion, high temperature and shocks under varying speed, they gradually degrade from a normal/health condition to a failure condition. Usually, the degradation process over the whole lifetime of the bearings can be classified into two phases: (1) phase I-normal phase and (2) phase II-significant degradation phase. For example, the bearing health indicator for

processing three sets of accelerated bearing degradation data is plotted in Fig. 1, where it is observed that different bearings have different degradation rates and failure times.

In phase I, the bearing health indicator has very small amplitudes and stays at a stable level, which reflects that a bearing is in a normal/health condition. In phase II, the bearing health indicator exhibits an exponential degradation trend with amplitude. In recent years, several time-frequency features such as root-mean-square (RMS), Kurtosis, crest value, RMS entropy estimator (RMS-EE) [8] and frequency spectrum partition summation (FSPPS), etc., extracted from vibration signals for bearing degradation tracking were reported in the previous researches. Based on the obtained health indicators, various prediction models were also proposed for

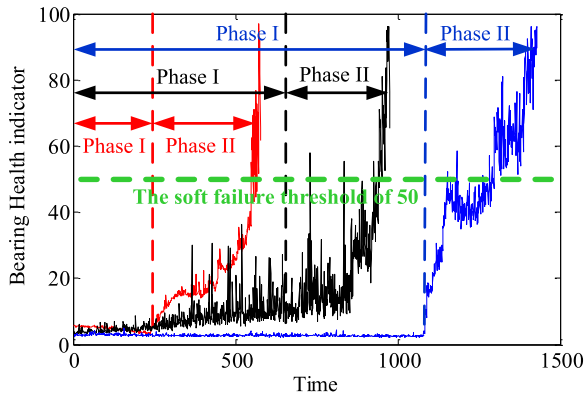


FIGURE 1. Typical bearing degradation trends described by the bearing health indicator.

estimating the health status of the rolling bearings. Current existing prediction approaches can be classified into three categories: physics-based models, knowledge-based methods and data-driven prediction models.

For physics-based models, for example, Fatigue crack growth (FCG) model [9] and Fatigue spall progression life (FSPL) model [10], which describe the evolution of structural damage according to the physical mechanisms. However, the limitation in developing physics-based prediction models is that they require extensive historical defect data collected by sensors beforehand. Besides, once a physics-based model is established, the relevant model parameters cannot be adjusted, which means that the actual degeneration in running states as reflected in the measured signals will not be utilized in real time [11], [12]. In comparison, the knowledge-based prediction methods such as neural network [13], deep learning [14], [15], expert system [16], etc., which take advantages of prior empirical knowledge. Although the forecasting accuracy is greatly improved in terms of probabilistic distributions, those approaches still need require a larger number of historical samples to form a training model. On the other hand, state-of-the-art knowledge-based prognostic techniques typically rely on empirical knowledge and more suitable for qualitative evaluation, the quantitative prediction in practical applications still needs to be improved [17]. Data-driven prediction models such as hidden Markov model (HMM) [18], time series model [19], [20], support vector machine (SVM) [21], [22], etc., which are not establish complex prediction equations at the initial analytical stage, and the model parameters can be adjusted to capture the degradation trend of vibration signals. In addition, both quantitative results and probabilistic distributions of the predicted data can be obtained by data-driven methods, meanwhile, different kinds of physical knowledge of the system cannot be integrated. A disadvantage associated with these data-driven techniques is that they may be applicable to the mechanical system under specific operation condition, might not work when the operating conditions of the system are changed [23], [24].

Over the past years, the self-similarity (SS) and fractional order characteristic (FOC) of health indicators series

aroused great interest and have become increasingly popular in the field of forecast applications. For example, in [25], Li et al. proposed a long range dependence (LRD) prediction approach called adaptive fractional autoregressive integrated moving average (f -ARIMA) to investigated the running tendency of rolling bearing based on equivalent vibration intensity (EVI) health factor. Li and Li [26], [27], demonstrated the suitability of prediction method based on long range dependence and short range dependence (SRD) and fractal time series of fractional system. Song *et al.* [28], developed a minimum entropy deconvolution and fractional Brownian motion degradation model to predict the bearing running tendency during a serious fault condition. Although self-similarity and FOC property can be observed in a wide range of mechanical operation systems, and some good prediction results were obtained by the fractional models, however, there are two potential problems related the above literatures still remained unresolved.

(1) In self-similarity and FOC domain, the Hurst exponent (HE) plays a significant role in the prediction of fractional systems. There are many methods to estimate the HE, including the maximum likelihood estimation and rescaled range analysis (R/S), local Whittle's estimator (LWE), wavelet based method [29]–[31], etc. However, the calculation of HE by classical estimator technique is sensitive to the length of the profile, non-stationary characteristic and noise, for example, the R/S statistic model was shown to be sensitive to heteroskedasticity and short-range dependence in the underlying process, leading to the prediction accuracy reduced dramatically if the Hurst exponent lack of the optimal solution.

(2) For the case that some sharp transition points (STPs, or abrupt change points) are contained in the health indicator time series, especially the time series at the junction between the phase I and phase II, as shown in Fig.1, if we applying the conventional fractional systems models to process those special points/sequences, the accuracy of the prediction will be fallen dramatically.

To overcome these unresolved limitations and improve prediction accuracy, in this paper, a novel approach based on improved R/S statistic model and fractional Brownian motion (FBM) for rolling bearings degradation prognostics is proposed. The sensitive issue related to heteroskedasticity and short-range dependence in the underlying process will be addressed by the improved R/S statistic technique with autocovariance estimator. The STPs problem will be solved by the new stochastic differential equation (SDE) which combined FBM with Brownian motion. Further, we show how to calculate the drift and volatility parameters of the SDE predicting operator to obtain a reliable prediction result. Results of accelerated life test indicate that significant improvements in prediction accuracy are obtained with the proposed model compared to the persistence methods.

The layout of this paper is organized as follows. Section 2 introduces the algorithm and theoretical derivation of the fractional Brownian motion and stochastic

differential equation. Section 3 describes the model of improved R/S statistic technique. In section 4, the bearing degradation process prognostic results and discussion of the proposed algorithm with other approaches previously are investigated. Conclusions are presented in Section 5.

II. FRACTIONAL BROWNIAN MOTION AND STOCHASTIC DIFFERENTIAL EQUATION

A. RANDOM WALK AND BROWNIAN MOTION

Let $X(t)$ be a stochastic process (random process) and its collection is $\{X(t)\}$, the mean of the process is as follows:

$$\mu(t) = E[X(t)] \tag{1}$$

and the auto-covariance of the stochastic process can be defined as,

$$r(s, t) = Cov[X(s), X(t)] = E[(X(s) - E(X(s)))(X(t) - E(X(t)))] \tag{2}$$

Furthermore, for a stochastic process $X(t)$, divide the time into n intervals with a fixed-length Δt , correspondingly, if we divide a space into n intervals with a fixed-length, we have,

$$\Delta x = \sigma \sqrt{\Delta t} \tag{3}$$

Assign a random variable ξ is ± 1 with probabilities 0.5, i.e., $p(\xi = -1) = 0.5 = p(\xi = 1)$, for $t = \Delta t$, the random walk W_t can be defined by,

$$W_t = \xi_1 \Delta x + \xi_2 \Delta x + \dots + \xi_n \Delta x \tag{4}$$

If $n \rightarrow \infty$, and thus $\Delta t \rightarrow 0$ with $t = n\Delta t$ is fixed, the result is called the Brownian motion model (BM), denoted as $B(t)$. Mathematically, random walk W_t has zero mean value and its variance is $n(\Delta x)^2 = \sigma^2 t$. It is easy to find that $B(t)$ has zero mean value and its variance $\sigma^2 t$. Generally, for a stochastic process $X(t)$ which satisfies $E[X(t)] = 0$ and $Var(X(t)) = \sigma^2$, the random walks can be embedded into Brownian motion. The idea is that, if we define a sequence $t_1 < t_2 < \dots < t_n$ of stopping times, the random walks sequence $\{W_n, n > 1\}$ can be expressed as $W_n = B(t_n)$ with increments distributed like stochastic process $X(t)$. Furthermore, the trajectories of random walk converge in distribution to Brownian motion trajectories (it is the result of the invariance principle [32]), which states that, for the random walk sequence $\{W_n, n > 1\}$ with zero mean value and variance $Var(X(t)) = \sigma^2$, then the Brownian motion $B(t_n)$ defined with $B(t_n) = \frac{1}{\sigma\sqrt{n}} \sum_{k=1}^n W_k$ [33]. The auto-covariance between $B(t_1)$ and $B(t_2)$ is $E[B(t_1)B(t_2)] = \min(t_1, t_2)$, which can be derived as follow:

For Brownian motion $B(t)$, the probability of the sequence $\{B(t_1), B(t_2), \dots, B(t_n)\}$ is given by [34],

$$P_n(X) = [(2\pi)^n t_1(t_2 - t_1)(t_3 - t_2) \dots (t_n - t_{n-1})]^{-\frac{1}{2}} \times \int_X e^{-\frac{1}{2}[\frac{x_1^2}{t_1} + \frac{(x_2 - x_1)^2}{t_2 - t_1} + \dots + \frac{(x_n - x_{n-1})^2}{t_n - t_{n-1}}]} dx_1 \dots dx_n \tag{5}$$

Suppose $t < s$, then the inverse of the auto-covariance matrix satisfies,

$$(\Lambda x, x) = \frac{x_1^2}{t} + \frac{(x_2 - x_1)^2}{s - t} \tag{6}$$

where the matrix Λ is $\Lambda = \begin{bmatrix} \frac{s}{(s-t)t} & \frac{-1}{s-t} \\ \frac{-1}{s-t} & \frac{1}{s-t} \end{bmatrix}$, and $m = \Lambda^{-1} = \begin{bmatrix} t & \\ & ts \end{bmatrix}$, i.e., for $t < s$, it satisfies $m(t, t) = t$, $m(t, s) = t$, $m(s, t) = t$, $m(s, s) = s$. Thus, for all $t > 0$ and $s > 0$, we get $m(t, s) = \min(t, s)$.

B. FRACTIONAL BROWNIAN MOTION (FBM)

If the walks in which the steps are not independent, and each step depends on the previous steps (long-term or short-term historical steps), which called semi-random walks. Therefore, the fractional Brownian motion (FBM) is introduced by semi-random walks [35]–[39].

The fractional Brownian motion can be defined using the stochastic integral representation (Mandelbrot and Van Ness 1968),

$$B^H(t) = C_H \left\{ \int_{-\infty}^0 [(t-s)^{H-\frac{1}{2}} - (-s)^{H-\frac{1}{2}}] dB(s) + \int_0^t (t-s)^{H-\frac{1}{2}} dB(s) \right\} \tag{7}$$

where $B(t)$ is a standard Brownian motion, $H(0 < H < 1)$ is Hurst exponent (the detailed calculation processes of HE are given in section 3), and $B^H(t = 0) = 0$. The coefficient $C_H = \frac{\sqrt{2H} \sin(H\pi) \Gamma(2H)}{\Gamma(H+1/2)}$, in which $\Gamma(x) = \int_0^\infty \exp(-x) dx$ is the Gamma function. For a FBM process, $B^H(t)$ has the following properties:

- (1) $B^H(t)$ has continuity trajectory;
- (2) $B^H(t)$ is a Gaussian process and for all $t \geq 0, 0 < H < 1$, we have $E[(B^H(t))^2] = t^{2H}$;
- (3) For all $t \geq 0, B^H(0) = 0$ and $E[B^H(t)] = 0$;

It should be noted that the Brownian motion is a special case of FBM with Hurst parameter $H = 1/2$. The FBM is a time-varying process, but its increment process $B^H(t_2) - B^H(t_1)$ of FBM are a stationary process, which obeys a fractional Gaussian noise distribution. The increment $B^H(t_2) - B^H(t_1)$ is Gaussian distributed with the following properties:

- (1) Increment $B^H(t_2) - B^H(t_1)$ is normal;
 - (2) $E[B^H(t_2) - B^H(t_1)] = 0$;
 - (3) $[E(B^H(t_2) - B^H(t_1))]^2 = \sigma^2 c |t_2 - t_1|^{2H}$;
- where $c = [1/2H[\Gamma(H + 1/2)]^2]^{2H}$ is the proportionality constant. In addition, the covariance between $B^H(t_2)$ and $B^H(t_1)$ is as follows:

$$cov(B^H(t_2), B^H(t_1)) = \sigma^2(c/2)(t_2^{2H} + t_1^{2H} - |t_2 - t_1|^{2H}) \tag{8}$$

C. PREDICTING OPERATOR DRIVEN BY STOCHASTIC DIFFERENTIAL EQUATION (SDE)

In this section, the prognostics problem of solution of stochastic differential equation (SDE) with fractional Brownian

motion is presented. Let $\{X(t), t \geq 0\}$ be a stochastic process in complete probability space (Ω, \mathbf{F}, p) , which is the solution of the following formula,

$$\begin{cases} dX(t) = a(t)X(t)dt + dB^H(t) \\ X(0) = x_0 \end{cases} \quad (9)$$

where $x_0 \in R$, and a is bounded, $B^H(t)$ is a standard FBM, $0 < H < 1$. It's easy to calculate that $X(t)$ is given by,

$$X(t) = e^{\int_0^t a(s)ds} x_0 + \int_0^t e^{\int_s^t a(s)ds} dB^H(s) \quad (10)$$

The following proposition, lemmas and their derivations are the prediction for $B^H(t)$, which are given by,

Proposition 1: Let $\{X(t), t \geq 0\}$ be the stochastic process given by Eq.(10), which is the solution of Eq.(9). For $t > 0$ and $s \in (0, t)$ be fixed, we have the following equality,

$$\begin{aligned} E[X(t)|X(r), r \in [0, s]] &= e^{\int_s^t a(s)ds} X(s) + \int_0^s u_{-(H-\frac{1}{2})} \\ &\times (I_{-s}^{-(H-\frac{1}{2})} (I_{-t}^{H-\frac{1}{2}} u_{H-\frac{1}{2}} \cdot v \cdot 1_{[s,t]})) dB^H \\ &= e^{\int_s^t a(s)ds} X(s) + \int_0^s u_{-(H-\frac{1}{2})} \\ &\times (I_{-s}^{-(H-\frac{1}{2})} (I_{-t}^{H-\frac{1}{2}} u_{H-\frac{1}{2}} \cdot v \cdot 1_{[s,t]})) d(X - aXdr) \end{aligned} \quad (11)$$

where $u_a(r) = r^{(a)}$ and $v(r) = e^{\int_r^t a}$.

Lemma 1: If $0 < s < t$, and c is an element of L_H^2 , we have,

$$\begin{aligned} E \left[\int_s^t cdB^H \mid B^H(r), r \in [0, s] \right] &= \int_0^s u_{-(H-\frac{1}{2})} (I_{-s}^{-(H-\frac{1}{2})} (I_{-t}^{-(H-\frac{1}{2})} u_{H-\frac{1}{2}} c)) dB^H \end{aligned} \quad (12)$$

Proof: For $t > 0$ and $s \in [0, t]$, by the result in Pipiras and Taqqu [40],

$$\begin{aligned} E \left[B^H(t) \mid B^H(r), r \in [0, s] \right] &= B^H(s) + \int_0^s u_{-(H-\frac{1}{2})} (I_{-s}^{-(H-\frac{1}{2})} (I_{-t}^{H-\frac{1}{2}} u_{H-\frac{1}{2}} 1_{[s,t]})) dB^H \end{aligned} \quad (13)$$

To validate Eq.(12), we assume that c is a step function, and we have

$$c(r) = \sum_{i=0}^{n-1} c_i 1_{[t_i, t_{i+1})}(r) \quad (14)$$

For $r \in [s, t)$, in which $s = t_0 < t_1 < \dots < t_n = t$, so the integral of $c(r)$ is given by,

$$\int_s^t cdB^H = \sum_{i=0}^{n-1} c_i (B^H(t_{i+1}) - B^H(t_i)) \quad (15)$$

Furthermore, we have,

$$\begin{aligned} E \left[\int_s^t cdB^H \mid B^H(r) \right] &= \int_0^s u_{-(H-\frac{1}{2})} (I_{-s}^{-(H-\frac{1}{2})} \\ &\times (I_{-t}^{H-\frac{1}{2}} u_{H-\frac{1}{2}} \sum_{i=0}^{n-1} c_i (1_{[t_0, t_{i+1})} - 1_{[t_0, t_i]})) dB^H \\ &= \int_0^s u_{-(H-\frac{1}{2})} (I_{-s}^{-(H-\frac{1}{2})} (I_{-t}^{H-\frac{1}{2}} u_{H-\frac{1}{2}} \sum_{i=0}^{n-1} c_i 1_{[t_i, t_{i+1})})) dB^H \end{aligned} \quad (16)$$

Then, it follows from Eq. (12) that,

$$\begin{aligned} E \left[\int_0^t cdB^H \mid B^H(r), r \in [0, s] \right] &= \int_0^s cdB^H + E \left[\int_s^t cdB^H \mid B^H(r), r \in [0, s] \right] \end{aligned} \quad (17)$$

where $c \in L_H^2$, and the error variance (EV) for the prediction of $\int_0^t cdB$ is given

$$EV = \int_s^t (u_{-(H-\frac{1}{2})}(r) (I_{-t}^{H-\frac{1}{2}} u_{H-\frac{1}{2}} c 1_{[s,t]}(r)))^2 dr \quad (18)$$

As a matter of fact, the above EV follows the fact that $E[(\int_0^t cdB^H)^2] = |c|_H^2$. The above lemma 1 provides a prediction result for the solution Eq.(10) of Eq.(9).

In addition to the stochastic differential equation (SDE) in Eq.(9), many improved and optimized SDE models were proposed, for example, the stochastic Langevin differential equation [41], as follow,

$$\begin{cases} dX(t) = a(t)X(t)dt + b(t)dB^H(t) \\ X(0) = x_0 \end{cases} \quad (19)$$

and geometric fractional Brownian motion [42]:

$$\begin{cases} dX(t) = X(t)(a(t)dt + b(t)dB^H(t)) \\ X(0) = x_0 \end{cases} \quad (20)$$

where $a(t)$ and $b(t)$ denote the drift and volatility parameters of the underlying, respectively.

The aim of this section is to obtain the predicting operator formulas for sharp transition points (STPs) based on stochastic differential equation, in the paper, a new stochastic differential equation is introduced, that is,

$$\begin{cases} dX(t) = aX(t)dt + bX(t)d[\varepsilon B(t) + B^H(t)] \\ X(0) = x_0 \end{cases} \quad (21)$$

where parameter ε denote constant, $B^H(t)$ is a standard FBM, $B(t)$ is a standard BM. We rewrite the above equation as,

$$dX(t) = aX(t)dt + \varepsilon bX(t)dB(t) + bX(t)dB^H(t) \quad (22)$$

Lemma 2: Parameter α and σ are constant, the stochastic differential equation,

$$dX(t) = \alpha X(t)dB(t) + \sigma X(t)dt \quad (23)$$

Its solution can be given by:

$$X(t) = X(0) \exp[\alpha B(t) + (\sigma - \frac{\alpha^2}{2})t] \quad (24)$$

Proof: Rewrite the Eq. (23) as,

$$\frac{dX(t)}{X(t)} = \alpha dB(t) + \sigma dt \quad (25)$$

Taking integration on the both sides of Eq. (25), we can get,

$$\int_0^t \frac{dX(t)}{X(t)} = \int_0^t \alpha dB(t) + \int_0^t \sigma dt = \alpha B(t) + \sigma t \quad (26)$$

According to the Ito's formula [43], we have,

$$df(t, X(t)) = \frac{\partial f}{\partial t} f(t, X(t))dt + \frac{\partial f}{\partial x} f(t, X(t))dX(t) + \frac{1}{2} \frac{\partial^2 f}{\partial x^2} f(t, X(t))(dX(t))^2 \quad (27)$$

Taking $f(t, x) = f(x) = \ln x$, then, $f'(x) = \frac{1}{x}, f''(x) = -\frac{1}{x^2}$. Then,

$$\begin{aligned} d \ln(X(t)) &= \frac{1}{X(t)} dX(t) - \frac{1}{2} \frac{1}{X^2(t)} (dX(t))^2 \\ &= \frac{1}{X(t)} dX(t) - \frac{1}{2} \alpha^2 dt \end{aligned} \quad (28)$$

i.e.,

$$\ln(X(t)) - \ln(X(0)) = \int_0^t \frac{dX(u)}{X(u)} - \frac{\alpha^2 t}{2} \quad (29)$$

Let combine Eq. (29) and Eq. (26), we have,

$$\ln \left(\frac{X(t)}{X(0)} \right) + \frac{\alpha^2 t}{2} = \int_0^t \frac{dX(u)}{X(u)} = \alpha B(t) + \sigma t \quad (30)$$

Thus the solution of Eq. (23) can be obtained, i.e., $X(t) = X(0) \exp[\alpha B(t) + (\sigma - \frac{\alpha^2}{2})t]$.

Lemma 3: Parameter α and σ are constant, the stochastic differential equation,

$$\begin{cases} dX(t) = \alpha X(t)dB(t) + \sigma X(t)dB^H(t) \\ X(0) = x_0 \end{cases} \quad (31)$$

and its solution can be given by:

$$X(t) = X(0) \exp(\alpha B(t) + \sigma B^H(t) - \frac{1}{2} \alpha^2 t) \quad (32)$$

Let's return Eq. (21) and Eq. (22), taking integration on the both sides of Eq. (22), we can get,

$$X(t) = X(0) + \int_0^t \alpha X(s)ds + \varepsilon b \int_0^t X(s)dB(s) + b \int_0^t X(s)dB^H(s) \quad (33)$$

where parameter ε and b denote constants. Let the coefficients of Eq. (31) satisfy assumption [43, Th. 3.2.3], according to the results of Lemma 2 and Lemma 3, the solution of Eq. (21) can be coarsely expressed as,

$$X(t) = X \exp[at + b(B^H(t) + \varepsilon B(t))] \quad (34)$$

where definite $Y(t) = at + b(B^H(t) + \varepsilon B(t))$. Since the $dB(t) = \omega_1(t)dt, dB^H(t) = \omega_2(t)(dt)^H$, and if the time $[0, T]$ is divided into N equal interval, i.e., $t_0, t_1, t_2, \dots, t_N$, the interval length is $h = T/N$, thus the increment in Eq. (21) can be discretized as

$$\begin{aligned} dX(t) &= \alpha X(t)dt + bX(t)d\varepsilon B(t) + bX(t)dB^H(t) \\ \Rightarrow \Delta X &= a \cdot X(t) \cdot \Delta t \\ &+ b \cdot X(t) \cdot \varepsilon \cdot \omega_1(t) \cdot \Delta t + b \cdot X(t) \cdot \omega_2(t) \cdot (\Delta t)^H \end{aligned} \quad (35)$$

where $\Delta X = X(t_{j+1}) - X(t_j), j = 1, 2, \dots, N$.

If we assuming the interval is h , thus $t = (h, 2h, \dots, Nh)'$, $B(t) = [B_h(t), B_{2h}(t), \dots, B_{Nh}(t)]'$ and $B^H(t) = [B_h^H(t), B_{2h}^H(t), \dots, B_{Nh}^H(t)]'$. Thus the joint probability density function (JPDF) of Y can be expressed by,

$$\begin{aligned} g(Y) &= (2\pi b^2)^{-\frac{N}{2}} |\Lambda_{H\varepsilon}|^{\frac{1}{2}} \\ &\times \exp\left(-\frac{1}{2b^2}(Y - at)' \cdot \Lambda_{H\varepsilon}^{-1} \cdot (Y - at)\right) \end{aligned} \quad (36)$$

where

$$\begin{aligned} \Lambda_{H\varepsilon} &= \left[cov[B_{ih}^H(t) + \varepsilon B_{ih}(t), B_{jh}^H(t) + \varepsilon B_{jh}(t)] \right]_{i,j=1,2,\dots,N} \\ &= \varepsilon^2 h(i \wedge j)_{i,j=1,2,\dots,N} + \frac{1}{2} h^{2H} (i^{2H} + j^{2H} - |i-j|^{2H})_{i,j=1,2,\dots,N} \end{aligned}$$

Then we get the Logarithmic likelihood function of $g(Y)$ is,

$$\begin{aligned} \ln g(Y) &= -\frac{N}{2} \ln(2\pi b^2) - \frac{1}{2} \ln |\Lambda_{H\varepsilon}| \\ &- \frac{1}{2b^2} (Y - at)' (Y - at)' \end{aligned} \quad (37)$$

The maximum likelihood estimating function of a and b can be calculated by taking the partial derivatives, we have,

$$\hat{a} = \frac{t' \Lambda_{H\varepsilon}^{-1} Y}{t' \Lambda_{H\varepsilon}^{-1} t} \quad (38)$$

$$\hat{b} = \frac{1}{N} \cdot \frac{(Y' \Lambda_{H\varepsilon}^{-1} Y)(t' \Lambda_{H\varepsilon}^{-1} t) - (t' \Lambda_{H\varepsilon}^{-1} Y)^2}{t' \Lambda_{H\varepsilon}^{-1} t} \quad (39)$$

III. IMPROVED R/S STATISTIC MODEL

The HE plays a significant role in the prediction of fractional Brownian motion. Hurst exponent, $0 < H < 1$, which is used for testing long-range dependence characteristic for a stochastic process an autocorrelation function $\rho(k)$ decaying as $\rho(k) \propto k^{2H-2}$ with a lag $k \rightarrow \infty$, and higher Hurst value indicating a smoother trend, less volatility, and less roughness. There are many methods to estimate the HE, including the maximum likelihood estimation and rescaled range analysis, local Whittle's estimator, wavelet based method, etc. Generally, the Hurst exponent directly determines the path trajectory of the FBM, and thus the value of Hurst exponent reflects the types of bearing degradation tendency which can be characterized by corresponding FBM model. However, the estimation algorithms of Hurst exponent are usually either

biased or exhibits fluctuate substantially for finite samples as shown in previous researches [44]–[46]. For example, the rescaled range analysis (R/S) statistic estimator is a classical method for Hurst exponent [29]–[31]. Although the R/S statistic estimator has been successfully applied to a number of time series such as economic time series, geological events and long-term weather records, etc., however, the calculation of HE by R/S statistic estimator technique is sensitive to the length of the profile, non-stationary characteristic and noise. For a stochastic process $X(t)$, the R/S statistic estimator can be expressed by,

$$\frac{R(n)}{S(n)} = \frac{1}{S(n)} \left\{ \begin{array}{l} \max \sum_{i=1}^n [X(t_i) - \frac{1}{n} \sum_{i=1}^n X(t_i)] \\ - \min \sum_{j=1}^n [X(t_j) - \frac{1}{n} \sum_{j=1}^n X(t_j)] \end{array} \right\} \quad (40)$$

where $R(n)$ is the range in each segment and $S(n)$ is the standard deviation, i.e., $S(n) = \sqrt{\frac{1}{n} \sum_{i=1}^n (X(t_i) - \frac{1}{n} \sum_{i=1}^n X(t_i))^2}$. The Hurst exponent H is deduced from the fitted straight line of $\log(R(n)/S(n))$ vs $\log(S(n))$. Generally speaking, we have the following conclusions:

In particular, (1) the case $0 < H < 0.5$, yields negatively correlated increments, the time series $X(t)$ belongs a short-range dependence (SRD) process, the self-similar correlation shows anti-persistent behavior; (2) the case $H=0.5$, yields the standard Brownian motion, the self-similar correlations are random and uncorrelated; On the other hand, (3) the case $0.5 < H < 1$, yields positively correlated increments, the time series $X(t)$ exhibits a long-range dependence process, the self-similar correlation shows persistive correlations behavior, i.e. trend reinforcing. The FBM with such H is used when slowly decaying effects are observed, in which the past events have a decaying effect on the future.

Due to the vibration signals of rotating machinery belong to non-stationary and non-Gaussian time series, the classical R/S statistic estimator may generate great fluctuation, especially during the serious failure status of rotating machinery. Meanwhile, the R/S statistic model was shown to be sensitive to heteroskedasticity and short-range dependence in the underlying process [47]. In this paper, the improved R/S (IR/S) statistic model is proposed to address this issue.

The improved R/S statistic model differs in the definition of the standard deviation $S(n)$, and the estimator $S^2(n)$ is defined as follows,

$$S^2(p) = \frac{1}{n} \sum_{i=1}^n [X(t_i) - \frac{1}{n} \sum_{i=1}^n X(t_i)]^2 + \frac{2}{n} \sum_{i=1}^p \omega_i(p) \left\{ \sum_{i=j+1}^n \left[X(t_i) - \frac{1}{n} \sum_{i=1}^n X(t_i) \right] \times \left[X(t_{i-j}) - \frac{1}{n} \sum_{i=1}^n X(t_i) \right] \right\}$$

$$= \sum_{i=1}^n [X(t_i) - \overline{X(t_i)}]^2 + \frac{2}{n} \sum_{i=1}^p \omega_i(p) \left[\sum_{i=j+1}^n [X(t_i) - \overline{X(t_i)}][X(t_{i-j}) - \overline{X(t_i)}] \right] = S^2(n) + 2 \sum_{j=1}^p \omega_i(p) \gamma_j \quad (41)$$

where $\omega_j(p) = 1 - \frac{j}{p+1}$, $p < n$, and γ_j is the auto-covariance estimator of $X(t)$.

Thus, it should be noted that the classical R/S statistic model is a special case of improved R/S statistic approach with $p = 0$. The estimator $S^2(n)$ involves not only sums of squared deviations of $X(t_i)$, but also includes its weighted auto-covariance estimator γ_j . Thus, the complete expression of the improved R/S statistic model is as follows:

$$IRS = \frac{R(n)}{S(p)} = \frac{1}{\sqrt{S^2(n) + 2 \sum_{j=1}^p \omega_i(p) \gamma_j}} \left\{ \begin{array}{l} \max \sum_{i=1}^n [X(t_i) - \frac{1}{n} \sum_{i=1}^n X(t_i)] \\ - \min \sum_{j=1}^n [X(t_j) - \frac{1}{n} \sum_{j=1}^n X(t_j)] \end{array} \right\} \quad (42)$$

It should be noted that the classical R/S statistic model is a special case of improved R/S statistic approach with $p = 0$. The different part between R/S model and IRS model mainly focus on denominator. Next, the relationship between R/S and IRS will be illustrated by the distribution V of a Brownian bridge [48]. For a stochastic process $X(t)$, we have the following definition,

$$B_n(\tau) = \frac{1}{S(p)\sqrt{n}} S_{[n\tau]}, \tau \in [0, 1] \quad (43)$$

where $S_{[n\tau]}$ denotes the sum of zero mean random variable, i.e., $S_{[n\tau]} = \sum_{i=1}^{[n\tau]} \varepsilon_i$, and $[n\tau]$ represents the value $[n\tau]$ less than or equal to $n\tau$, and $B_n(\tau)$ is Brownian motion. For a stochastic process $X(t)$, we have the following theorem:

- (a) $\left\{ \max_{1 \leq i \leq n} \frac{1}{S(p)\sqrt{n}} \sum_{i=1}^n [X(t_i) - \overline{X(t_i)}] \right\} \Rightarrow \max_{0 \leq \tau \leq 1} B^o(\tau) = M^o$
- (b) $\left\{ \min_{1 \leq i \leq n} \frac{1}{S(p)\sqrt{n}} \sum_{i=1}^n [X(t_i) - \overline{X(t_i)}] \right\} \Rightarrow \min_{0 \leq \tau \leq 1} B^o(\tau) = m^o$
- (c) $\frac{1}{\sqrt{n}} RS \Rightarrow M^o - m^o = V$

The proofs for the above theorems are displayed in the [49] and [50]. Therefore, if the $\lim_{n \rightarrow \infty} E[\sum_{i=1}^n \frac{\varepsilon_i}{n}]$ is finite and positive,

and $\frac{1}{\sqrt{n}}RS \Rightarrow M^o - m^o = V$, then $\frac{1}{\sqrt{n}}IRS \Rightarrow \zeta V$, where,

$$\zeta = \sqrt{\frac{\lim_{n \rightarrow \infty} E[\frac{1}{n}(\sum_{i=1}^n \varepsilon_i)^2]}{\lim_{n \rightarrow \infty} E[\frac{1}{n} \sum_{i=1}^n \varepsilon_i^2]}} \quad (44)$$

The crucial issue of the new standard deviation measure is the number of lag p which is used for improved R/S statistic estimation, however, the lag p cannot be chosen too much lower because the auto-covariance estimator γ_j may be beyond the lag p substantially and the estimates of rescaled ranges and Hurst exponent are still biased; if the chosen lag is much higher, the estimates of the rescaled range differ significantly from the true values. In this paper, the optimal lag p can be calculated by first-order autocorrelation coefficient $\rho(1)$ of the sub-interval. That is,

$$p^* = \left\lfloor \left(\frac{3h}{2} \right)^{\frac{1}{2}} \left(\frac{2\rho(1)}{1 - \rho(1)} \right)^{\frac{2}{3}} \right\rfloor \quad (45)$$

where symbol $\lfloor \cdot \rfloor$ is the nearest lower integer operator and h is the length of each sub-interval.

In this paper, a novel prognostics technique by using improved R/S statistic model and fractional Brownian motion approach is proposed for rolling bearing degradation trend analysis. The procedures of prognostics technique can be divided into six steps:

- (1) Collect the vibration data of bearing whole life-cycle.
- (2) Calculate bearing health indicators including RMS and EVI exponent of whole life-cycle, using the following formulas: $V_{rms} = \sqrt{\frac{1}{N} \sum_0^{N-1} v^2(n)}$ and $v_s = \sqrt{(\frac{\sum v_x}{N_x})^2 + (\frac{\sum v_y}{N_y})^2 + (\frac{\sum v_z}{N_z})^2}$. Based on time-domain amplitude, the degenerate running trends can be divided two phases, i.e., normal phase and significant degradation phase.
- (3) Randomly choose any health factor, for example, EVI exponent of whole life-cycle, which will be used as predicting samples.
- (4) Apply the improved R/S statistic technique to calculate the Hurst exponents of bearing whole life-cycle. Meanwhile, watch the range of obtained Hurst exponents from the normal/health condition to incipient failure stage.
- (5) If $0.5 < H < 1$, the predicting samples time series exhibits a long-range dependence process, the stochastic differential equation of FBM predicting operator with such H is used for rolling bearing degradation prognostics.
- (6) Comparative analysis with other start-of-the art methods.

The flow chart of the proposed bearing degradation trend prognostics technique is illustrated in Fig. 2.

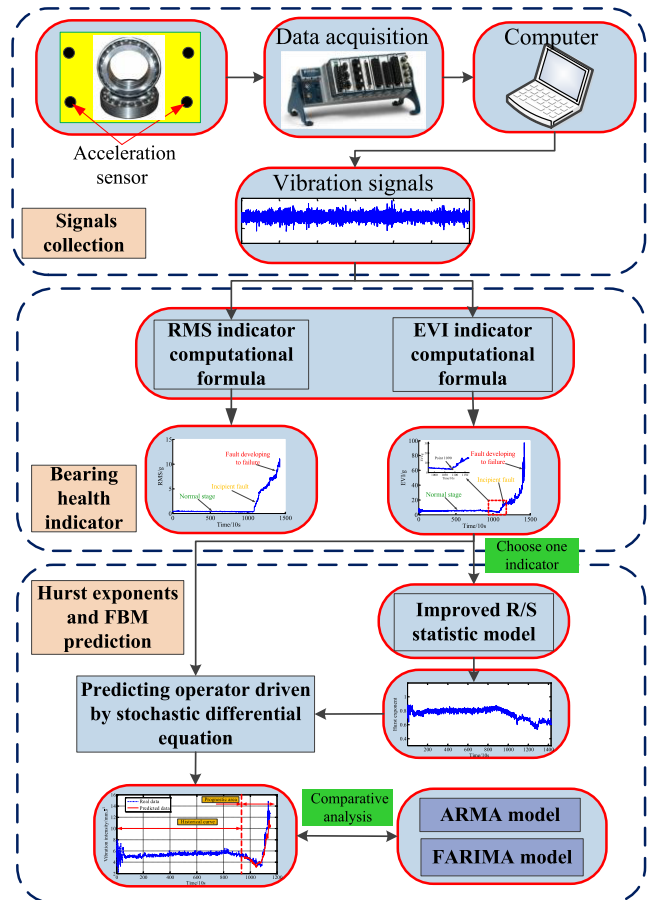
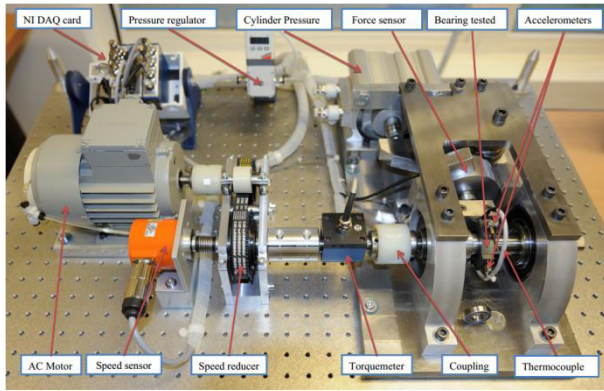


FIGURE 2. Flow chart of the proposed method for bearing degradation trend prognostics.

IV. EXPERIMENTAL EVALUATION

In order to validate effectiveness of the proposed method, experimental data from bearing accelerated life test were applied, as shown in Fig.3. The vibration data were collected by the IEEE prognostic and health management association [51]. The experimental platform including AC motor, tested bearing, speed sensor, accelerometers, torque-meter, thermocouple and NI-DAQ signal acquisition card, etc. For the vibration signals, the sampling frequency was set to 25.6 kHz, and 2560 sample points (i.e., 0.1s) were recorded each 10seconds. The authors analyzed the vibration acceleration data that this accelerated life test was carried out successively until the amplitude of vibration signal overpassed a certain level 20g. As shown in Fig.3, the severe wear failure in bearing ball and the spalling failure in inner race were observed after teardown.

Generally, the bearing degradation trend can be represented by some time-domain health indicators such as peak value, root-mean-square (RMS), vibration intensity (VI), Kurtosis and equivalent vibration intensity (EVI), etc., where the vibration intensity (VI) can only be partly described the running condition with one channel data, further, the EVIs could be calculated via three directions,



(a)



(b)

FIGURE 3. Overview of experimental setup and normal and degraded bearings [51]. (a) Overview of experimental setup; (b) Normal and degraded bearings.

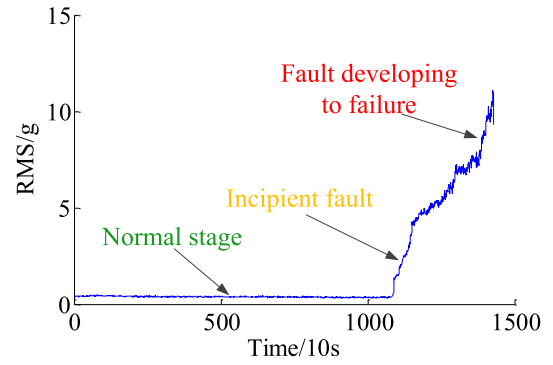
i.e., axis X-Y-Z, respectively. The EVI is defined as:

$$v_s = \sqrt{(\frac{\sum v_x}{N_x})^2 + (\frac{\sum v_y}{N_y})^2 + (\frac{\sum v_z}{N_z})^2}$$

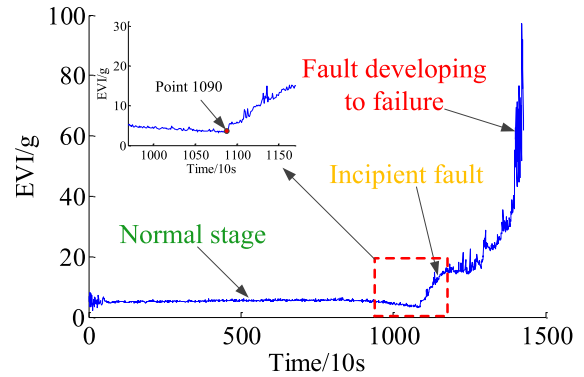
here V_x , V_y , and V_z are vibration intensity in axis X, Y, Z. In this paper, the RMS and EVI are discussed for further analysis. Fig.4 shows the root-mean-square (RMS) and equivalent vibration intensity (EVI) curves over the whole life-cycle of rolling bearing with 1428 points, and shows that there was a long time in stable or normal operation and the period in fault occurrence and severity is quite short. In this research, the health indicator EVI collected at incipient fault and serious failure stages was chosen as the target for degradation trend prognostics of rolling bearing. The evolution of EVI curve shows several areas of fluctuation which raises challenges for the prognostic task.

Fig. 5(a) and 5(b) show the curves of the lags p and the distribution of HE that calculated by improved R/S statistic model. From Fig. 5(b), it can be found that the self-similarity characteristic of EVI is strong in normal phase because the Hurst exponent are occurred between 0.6 and 1, i.e., $0.5 < H < 1$, and then the Hurst exponent values decline dramatically with the deterioration of the multiple faults. Moreover, it can be seen that the Hurst-based degradation curve has an opposite trend with the EVI curve, the fluctuation in the bearing degradation area (from incipient failure to serious failure) is also very large, resulting in that the prediction of EVI becomes more challenging.

In this work, the main concern for bearing prediction is that those degenerate trend points are covered from the



(a)



(b)

FIGURE 4. Time-domain health indicator feature waveforms of the rolling bearing. (a) RMS plot over whole lifetime; (b) EVI plot over whole lifetime.

normal/health condition to incipient failure stage, i.e., from phase I to phase II. From Fig.4 (b), it should be noted that some sharp transition points (STPs, which mean their vibration amplitudes are mutated sharply, e.g., point 1090 in Fig.4(b), or the Hurst exponent values are mutated rapidly, e.g., point 1090 in Fig.5(b)) are contained in the EVI time series, i.e., from 950 point to 1150point. The prediction from 950 point to 1150 point is divided into A to D stage, i.e., A: [950:1000], B: [1000:1050], C: [1050:1100], D: [1100:1150].The prediction curves of each stage for rolling bearing are illustrated in Fig. 6. The prediction data of different stages are integrated and compared with the original vibration data, the overall prediction results are shown in Fig. 7. As can be seen in Fig. 7, prediction data generated by FBM model is able to reasonably track the variation trend of original EVI.

In order to investigate the superiority of the proposed method, time series prognostics model ARMA and the f -ARIMA model that used in ref. [25] were employed to process and forecast the above tested data. The actual degradation data, prediction data generated by ARMA and the prediction data generated by f -ARIMA are presented in Fig. 8. As shown in Fig. 8, the ARMA and f -ARIMA prediction curves cannot exactly track the trend of degradation EVI points and has low estimation precision. The quantitative evaluations of the prognostic results using different methods are summarized in Table 1. It can be observed

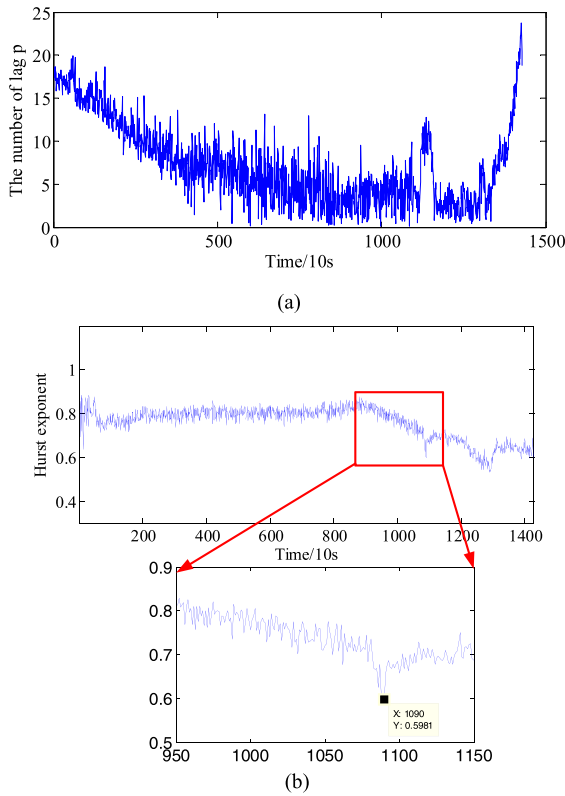


FIGURE 5. The results of improved R/S statistic method. (a)The curve of the number of lags p calculated by improved R/S statistic method; (b) Hurst curve over whole lifetime with improved R/S statistic method.

TABLE 1. The quantitative evaluations of the prognostic results using different methods.

| Index | FBM | ARMA | f -ARIMA |
|-----------------------------------|--------|---------|------------|
| Mean Absolute Error-MAE | 0.4489 | 1.0355 | 0.5424 |
| Average relative error-ARE | 0.0943 | 0.199 | 0.2799 |
| Root-Mean-Square Error-RMSE | 6.3640 | 14.6808 | 7.6894 |
| Normalized Mean Square Error-NMSE | 0.2414 | 5.6625 | 23.7229 |
| Maximum of Absolute Error-MaxAE | 5.6231 | 0.9647 | 9.9269 |

Note that: $MAE = \frac{1}{N} \sum_{k=1}^N |x(k) - \hat{x}(k)|$;

$ARE = \frac{1}{N} \sum_{k=1}^N \frac{|x(k) - \hat{x}(k)|}{x(k)}$; $RMSE = \sqrt{\sum_{k=1}^N \frac{1}{N-1} [x(k) - \hat{x}(k)]^2}$;

$NMSE = \frac{\sum_{k=1}^N [x(k) - \hat{x}(k)]^2}{\sum_{k=1}^N [x(k) - \overline{x(k)}]^2}$; $MaxAE = \max(|x(k) - \hat{x}(k)|)$.

from Table 1 that five quantitative indicators recorded by FBM approach are less than their corresponding values by other two methods. The comparison results indicate that the proposed FBM method can significantly improve the effectiveness and accuracy for bearing degradation trend tracking.

Here $x(k)$ and $\hat{x}(k)$ are actual data and predicted data, respectively.

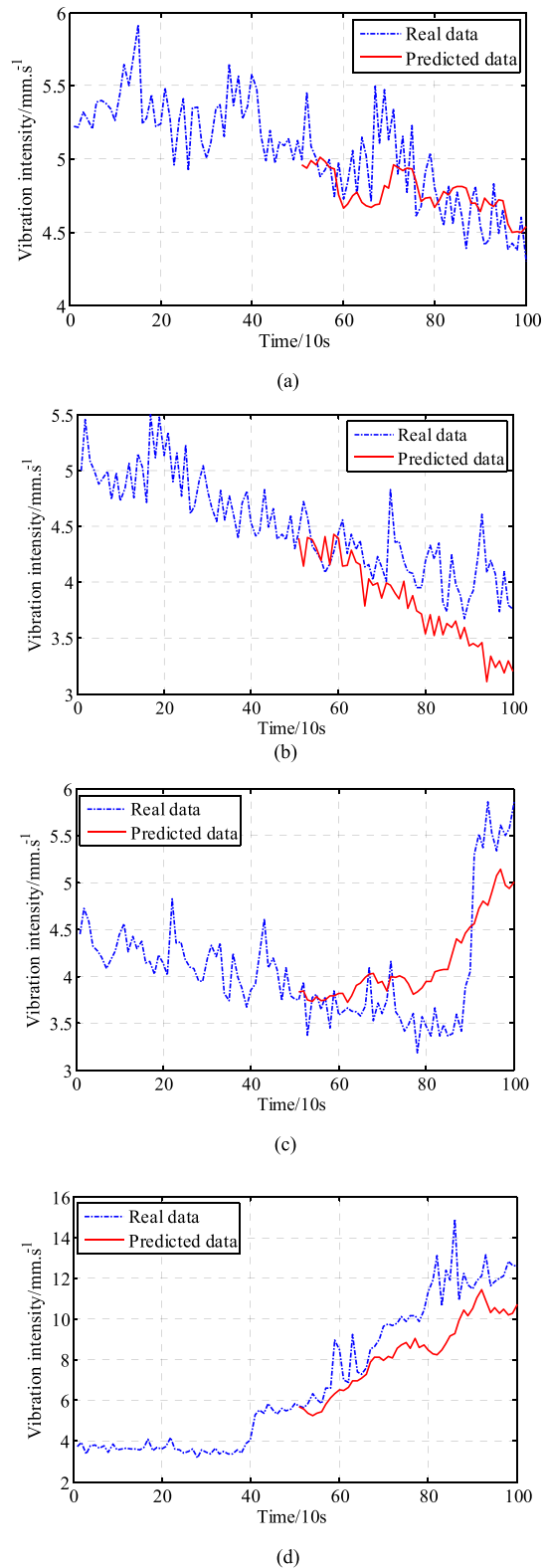


FIGURE 6. The prediction results by FBM in different sections. (a) The prediction result in stage A; (b) The prediction result in stage B; (c) The prediction result in stage C; (d) The prediction result in stage D.

Since the proposed prognostic algorithm considers the Hurst values are in range of 0.5 and 1, what has to be further discussed is what kind of Hurst scope is valid in FBM

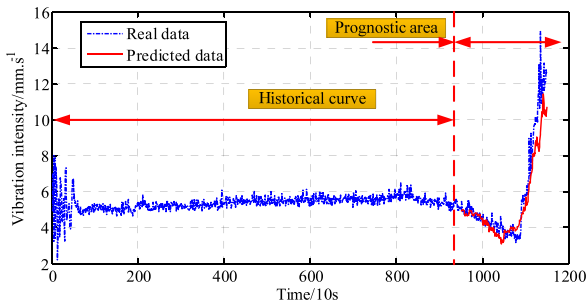


FIGURE 7. The actual data and the predicted data based on the FBM.

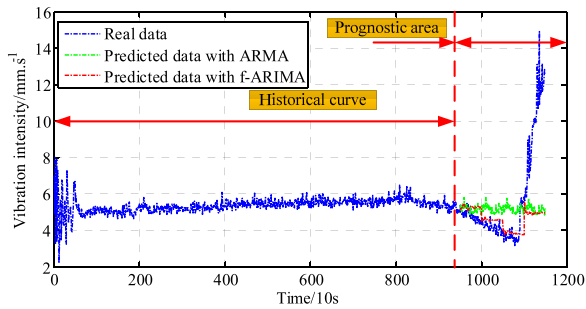


FIGURE 8. The actual and predicted data based on the ARMA model and the method in [25].

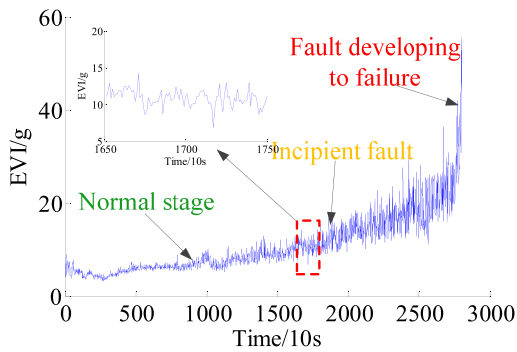


FIGURE 9. The EVI plot of the contrastive rolling bearing whole lifetime.

prognostic approach. Therefore, one of the most important boundary conditions, $H=0.5$ and $H=0.5$, should also be considered. For this purpose, another accelerated life test dataset of rolling bearing under the same operation was used. The whole life EVI results of contrastive (another) bearing is shown in Fig. 9. The corresponding Hurst exponents curve calculated by improved R/S statistic model is shown in Fig. 10, as can be seen, most of the Hurst exponents are lower than 0.5 from the phase I to phase II. Here, the time series from 1651 point to 1750 point is selected as a predicted sample. It can be seen from 1651 point to 1750 point that, lots of sample points less than or equal 0.5 are covered.

Accordingly, the FBM prediction results for [1651, 1700] and [1701, 1750] are shown in Fig. 11 (a) and 11(b), respectively. It is clear that the prediction accuracy of the proposed method is reduced greatly, it is also noted that most of

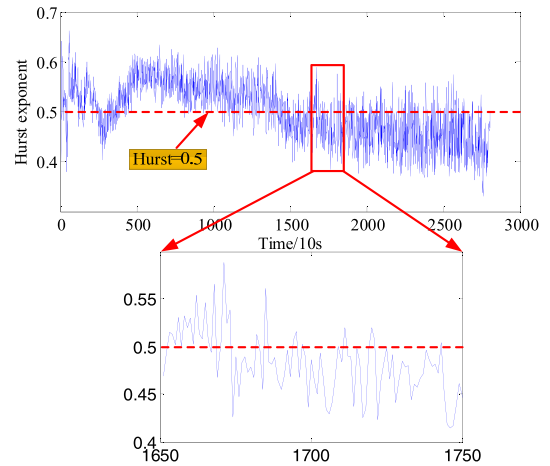


FIGURE 10. The Hurst curve of contrastive rolling bearing whole lifetime based on improved R/S statistic method.

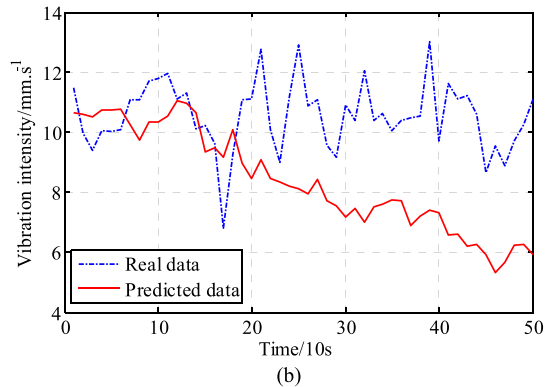
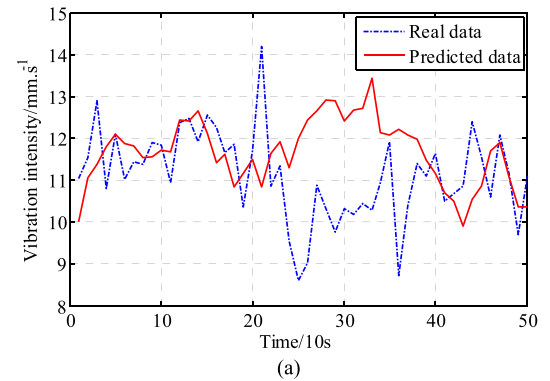


FIGURE 11. The actual data and the predicted data based on the FBM. (a) The prediction result for region [1651-1700]; (b) The prediction result for region [1701-1750].

predicted values deviate from the true values. Overall prediction performances are not satisfactory for bearing degradation trend, these results demonstrate that the proposed method cannot be applied efficiently for the time series with lower Hurst values, i.e., $H < 0.5$ and $H = 0.5$.

V. CONCLUSIONS

In this paper, a novel prognostics method based on fractional Brownian motion combined with improved R/S statistic technique is proposed for bearing degradation trends prognostics.

This research provides a good application direction based on self-similarity and fractional order characteristic theory. The proposed generalized R/S statistic model was applied to address the sensitive problems, i.e., the heteroskedasticity and short-range dependence of classical R/S statistic model. We introduced a new stochastic differential equation predicting operator combined Brownian motion with fractional Brownian motion. We also derive a computationally efficient algorithm using the maximum likelihood estimating technique for drift and volatility parameters of the SDE. Through analysis and validation the developed method can be effectively used for tracking bearings degradation related multiple faults in accelerated life test, the fault degradation from normal condition to incipient fault was considered particularly, and achieve a high prognostic accuracy.

The prognostic results show that the degradation tendency of rolling bearing can be effectively tracked, and some schemes similar to rolling bearing failure could be addressed by the proposed method. However, in practical application, some problems are also exposed: (1) the proposed algorithm is designed for detecting the bearing fault with the case of $0.5 < H < 1$, thus the Hurst values of vibration data, which are not covered in this range might failed in terms of prediction accuracy. (2) Acceleration sensor with one point location was designed and analyzed in this paper, in practical application, the degradation tendency of rolling bearing should be detected by multiple sensors with multi-point location, and each sensor should be supervised by a separate fractional Brownian motion model. (3) the proposed methodology is only applicable for accelerated life test of the bearings under constant operating conditions, the variable conditions such as variable speed, torque and variable harsh working environments should be considered in the future which may help generalizing the proposed method, and hope to enable further application to the preventive maintenance of other mechanical systems for preventive maintenance in the industries such as coal mining, well drilling and high-speed train, etc..

REFERENCES

- [1] D. Wang and K.-L. Tsui, "Two novel mixed effects models for prognostics of rolling element bearings," *Mech. Syst. Signal Process.*, vol. 99, pp. 1–13, Jan. 2018.
- [2] Q. Li, S. Y. Liang, and W. Song, "Revision of bearing fault characteristic spectrum using LMD and interpolation correction algorithm," *Proc. CIRP*, vol. 56, pp. 182–187, Dec. 2016.
- [3] A. Rezaei and A. Dadouche, "Development of a turbojet engine gearbox test rig for prognostics and health management," *Mech. Syst. Signal Process.*, vol. 33, pp. 299–311, Nov. 2012.
- [4] Q. Li, X. Ji, and S. Y. Liang, "Incipient fault feature extraction for rotating machinery based on improved AR-minimum entropy deconvolution combined with variational mode decomposition approach," *Entropy*, vol. 19, no. 7, p. 317, 2017.
- [5] D. L. Nuñez and M. Borsato, "An ontology-based model for prognostics and health management of machines," *J. Ind. Inf. Integr.*, vol. 6, pp. 33–46, Jun. 2017.
- [6] L. Saidi, "The deterministic bispectrum of coupled harmonic random signals and its application to rotor faults diagnosis considering noise immunity," *Appl. Acoust.*, vol. 122, pp. 72–87, Jul. 2017.
- [7] Y. Peng, J. Cheng, Y. Yang, and B. Li, "Adaptive sparsest narrow-band decomposition method and its applications to rotor fault diagnosis," *Measurement*, vol. 91, pp. 451–459, Sep. 2016.
- [8] J. B. Ali, B. Chebel-Morello, L. Saidi, S. Malinowski, and F. Fnaiech, "Accurate bearing remaining useful life prediction based on Weibull distribution and artificial neural network," *Mech. Syst. Signal Process.*, vols. 56–57, pp. 150–172, May 2015.
- [9] Y.-S. Shih and J.-J. Chen, "Analysis of fatigue crack growth on a cracked shaft," *Int. J. Fatigue*, vol. 19, no. 6, pp. 477–485, 1997.
- [10] Y. Choi and C. R. Liu, "Spall progression life model for rolling contact verified by finish hard machined surfaces," *Wear*, vol. 262, nos. 1–2, pp. 24–35, 2007.
- [11] Y. N. Qian, R. Q. Yan, and R. X. Gao, "A multi-time scale approach to remaining useful life prediction in rolling bearing," *Mech. Syst. Signal Process.*, vol. 83, pp. 549–567, Jan. 2017.
- [12] Y. Y. Jiang, Y. R. Wang, Y. Wu, and Q. Sun, "Fault prognostic of electronics based on optimal multi-order particle filter," *Microelectron. Rel.*, vol. 62, pp. 167–177, Jul. 2016.
- [13] L. Guo, N. Li, F. Jia, Y. Lei, and J. Lin, "A recurrent neural network based health indicator for remaining useful life prediction of bearings," *Neurocomputing*, vol. 240, pp. 98–109, May 2017.
- [14] J. Deutsch, M. He, and D. He, "Remaining useful life prediction of hybrid ceramic bearings using an integrated deep learning and particle filter approach," *Appl. Sci.*, vol. 7, no. 7, Jun. 2017, Art. no. 649.
- [15] J. Leng and P. Jiang, "A deep learning approach for relationship extraction from interaction context in social manufacturing paradigm," *Knowl.-Based Syst.*, vol. 100, pp. 188–199, May 2016.
- [16] M. S. Kumar and B. S. Prabhu, "Rotating machinery predictive maintenance through expert system," *Int. J. Rotating Mach.*, vol. 6, no. 5, pp. 363–373, 2000.
- [17] M. Mishra, J. Odelius, A. Thaduri, A. Nissen, and M. Rantatalo, "Particle filter-based prognostic approach for railway track geometry," *Mech. Syst. Signal Process.*, vol. 96, pp. 226–238, Nov. 2017.
- [18] J. Yu, "Adaptive hidden Markov model-based online learning framework for bearing faulty detection and performance degradation monitoring," *Mech. Syst. Signal Process.*, vol. 83, pp. 149–162, Jan. 2017.
- [19] J. Ma, F. Xu, K. Huang, and R. Huang, "GNAR-GARCH model and its application in feature extraction for rolling bearing fault diagnosis," *Mech. Syst. Signal Process.*, vol. 93, pp. 175–203, Sep. 2017.
- [20] H. T. Pham and B.-S. Yang, "Estimation and forecasting of machine health condition using ARMA/GARCH model," *Mech. Syst. Signal Process.*, vol. 24, no. 2, pp. 546–558, 2010.
- [21] S.-J. Dong, S.-R. Yin, B.-P. Tang, L.-L. Chen and T.-H. Luo, "Bearing degradation process prediction based on the support vector machine and Markov model," *Shock Vib.*, 2014, Art. no. 717465, doi: <http://dx.doi.org/10.1155/2014/717465>
- [22] P. Samui, "Prediction of pile bearing capacity using support vector machine," *Int. J. Geotech. Eng.*, vol. 5, no. 1, pp. 95–102, 2011.
- [23] M. S. Jha, G. Dauphin-Tanguy, and B. Ould-Bouamama, "Particle filter based hybrid prognostics for health monitoring of uncertain systems in bond graph framework," *Mech. Syst. Signal Process.*, vol. 75, pp. 301–329, Jun. 2016.
- [24] L. Ren, J. Cui, Y. Sun, and X. Cheng, "Multi-bearing remaining useful life collaborative prediction: A deep learning approach," *J. Manuf. Syst.*, vol. 43, pp. 248–256, Apr. 2017.
- [25] Q. Li, S. Y. Liang, J. Yang, and B. Li, "Long range dependence prognostics for bearing vibration intensity chaotic time series," *Entropy*, vol. 18, no. 1, p. 23, 2016.
- [26] M. Li, "Fractal time series—A tutorial review," *Math. Problems Eng.*, 2010, Art. no. 157264, doi: <http://dx.doi.org/10.1155/2010/157264>
- [27] M. Li and J.-Y. Li, "On the predictability of long-range dependent series," *Math. Problems Eng.*, 2010, Art. no. 397454, doi: <http://dx.doi.org/10.1155/2010/397454>
- [28] W. Song, M. Li, and J.-K. Liang, "Prediction of bearing fault using fractional Brownian motion and minimum entropy deconvolution," *Entropy*, vol. 18, no. 11, p. 418, 2016.
- [29] M. Garcin, "Estimation of time-dependent Hurst exponents with variational smoothing and application to forecasting foreign exchange rates," *Phys. A, Statist. Mech. Appl.*, vol. 483, pp. 462–479, Oct. 2017.
- [30] J.-F. Coeurjolly and E. Porcu, "Properties and Hurst exponent estimation of the circularly-symmetric fractional Brownian motion," *Stat. Probab. Lett.*, vol. 128, pp. 21–27, Sep. 2017.

- [31] L. Wu and Y. Ding, "Wavelet-based estimator for the Hurst parameters of fractional Brownian sheet," *Acta Math. Sci.*, vol. 37, no. 1, pp. 205–222, 2017.
- [32] P. Billingsley, "The invariance principle for dependent random variables," *Trans. Amer. Math. Soc.*, vol. 83, no. 1, pp. 250–268, 1956.
- [33] I. Karatzas and S. E. Shreve, *Brownian Motion and Stochastic Calculus*, 2nd ed. New York, NY, USA: Springer-Verlag, 1991.
- [34] I. M. Gelfand, *Generalized Functions*. San Francisco, CA, USA: Academic, 1977.
- [35] T. Sottinen and L. Viitasaari, "Prediction law of fractional Brownian motion," *Statist. Probab. Lett.*, vol. 129, pp. 155–166, Oct. 2017.
- [36] V. Bondarenko, V. Bondarenko, and K. Truskovskiy, "Forecasting of time data with using fractional Brownian motion," *Chaos Soliton. Fract.*, vol. 97, pp. 44–50, 2017.
- [37] J. Wen and Y. Shi, "Anticipative backward stochastic differential equations driven by fractional Brownian motion," *Statist. Probab. Lett.*, vol. 122, pp. 118–127, Mar. 2017.
- [38] M. Kamrani and N. Jamshidi, "Implicit Euler approximation of stochastic evolution equations with fractional Brownian motion," *Commun. Nonlinear Sci.*, vol. 44, pp. 1–10, Mar. 2017.
- [39] B. B. Mandelbrot and J. W. Van Ness, "Fractional Brownian motions, fractional noises and applications," *SIAM Rev.*, vol. 10, no. 4, pp. 422–437, 1968.
- [40] V. Pipiras and M. S. Taqqu, "Are classes of deterministic integrands for fractional Brownian motion on an interval complete?" *Bernoulli*, vol. 7, no. 6, pp. 878–897, 2001.
- [41] O. Baghani, "On fractional Langevin equation involving two fractional orders," *Commun. Nonlinear Sci. Numer. Simul.*, vol. 42, pp. 675–681, Jan. 2017.
- [42] L. Longjin, F.-Y. Ren, and W.-Y. Qiu, "The application of fractional derivatives in stochastic models driven by fractional Brownian motion," *Phys. A, Statist. Mech. Appl.*, vol. 389, pp. 4809–4818, Nov. 2010.
- [43] Y. Mishura, *Stochastic Calculus for Fractional Brownian Motion and Related Processes*. Berlin, Germany: Springer-Verlag, 2007.
- [44] J. Barunik and L. Kristoufek, "On Hurst exponent estimation under heavy-tailed distributions," *Phys. A, Statist. Mech. Appl.*, vol. 389, no. 18, pp. 3844–3855, 2010.
- [45] M. Couillard and M. Davison, "A comment on measuring the Hurst exponent of financial time series," *Phys. A, Statist. Mech. Appl.*, vol. 348, pp. 404–418, Mar. 2005.
- [46] L. Kriřtoufek, "Rescaled range analysis and detrended fluctuation analysis: Finite sample properties and confidence intervals," *AUCO Czech Econ. Rev.*, vol. 4, no. 3, pp. 315–330, 2010.
- [47] V. Alfi, F. Coccetti, M. Marotta, A. Petri, and L. Pietronero, "Exact results for the roughness of a finite size random walk," *Phys. A, Statist. Mech. Appl.*, vol. 370, no. 1, pp. 127–131, 2008.
- [48] T. Kariya, *Quantitative Methods for Portfolio Analysis: MTV Model Approach*. Norwell, MA, USA: Kluwer, 1993.
- [49] Y. A. Davydov, "The invariance principle for stationary processes," *Theory Probab. Appl.*, vol. 15, no. 3, pp. 487–489, 1970.
- [50] M. Taqqu, "Weak convergence to fractional Brownian motion and to the Rosenblatt process," *Zeitschrift Wahrscheinlichkeitstheorie Verwandte Gebiete*, vol. 31, no. 4, pp. 287–302, 1975.
- [51] P. Nectoux *et al.*, "PRONOSTIA: An experimental platform for bearings accelerated degradation tests," in *Proc. IEEE Int. Conf. Prog. Health Manage.*, Denver, CO, USA, Jun. 2012, pp. 1–8.



QING LI (GS'16) received the master's degree from the Shanghai University of Science and Engineering in 2015. He is currently pursuing the Ph.D. degree with the College of Mechanical Engineering, Donghua University, Shanghai. He is currently a Visiting Researcher with the Georgia Institute of Technology, Atlanta, GA, USA. He has authored in excess of 20 archival journal papers and professional conference articles in his research areas. His technical interests include dynamic signal/image processing, fault diagnosis for rotating machinery and machine learning, and so on. He is also an invited peer-reviewer for many prestigious international journals, such as *Material & Design*, the *Frontiers of Information Technology & Electronic Engineering*, and so on. In addition, he is a member of the American Society of Mechanical Engineers and the Vibration Engineering Society of China.



STEVEN Y. LIANG received the Ph.D. degree in mechanical engineering from the University of California at Berkeley in 1987. He was the Institute's founding Director of Precision Machining Research Consortium, the Director of Manufacturing Education Program, and the Associate Director of the Manufacturing Research Center from 1996 to 2008. He is currently a Professor (tenured) and the Morris M. Bryan, Jr. Professor in mechanical engineering for advanced manufacturing systems (permanently appointed) with the Georgia Institute of Technology. His technical interests include precision engineering, extreme manufacturing, and technology innovation. He is a fellow of ASME and the Society of Manufacturing Engineers International. He was a recipient of many prestigious awards, including the SME Robert B. Douglas Outstanding Young Manufacturing Engineer Award, the Society of Automotive Engineers Ralph R. Teetor Educational Award, the SME Blackall Machine Tool and Gage Award, and the Outstanding Alumni Award of National Cheng Kung University. He has been elected National Thousand-Elite Export of China and Shanghai Thousand-Elite Expert. He served as the President of the North American Manufacturing Research Institution and the Chair of the Manufacturing Engineering Division of The American Society of Mechanical Engineers.